

**Brookhaven National Laboratory**

**Brookhaven Science Associates**

**Upton, New York 11973**

***Muon g-2 Note No. 417***

**Title: Pulse Fitting in G2Too**

**Author: Fred Gray and Gerco Onderwater**

**Affiliation: University of Illinois**

**Date: September 5, 2002**

---



# Pulse fitting in G2Too

Fred Gray and Gerco Onderwater

September 5, 2002

## 1 Introduction

*MilliFit* is the name given to the pulse fitter in G2Too. It processes the raw samples recorded by the waveform digitizers into values of time and energy for each arriving positron. *MilliFit* uses information about the average pulse shape in each detector to separate pulses that arrive nearly simultaneously. It minimizes

### 3 Breaking up long islands

During periods with a high “flash” level, the signals from the stations located near the inflector exceeded the WFD hardware threshold for more than 100  $\mu$ s. It is impractical to fit all of the pulses residing on these continuous digitizations simultaneously: the number of fit parameters becomes too large, and the pedestal is no longer approximated well by a constant. Consequently, the island must be split up.

The first step in locating points at which it is safe to break the island is to estimate the pedestal as a function of time within the island. To do this, the island is broken into segments of up to 64 samples. Within each such interval, the pedestal is taken to be the average of the lowest few samples, where “few” is defined based on the RMS of the set of pedestal samples. The precise algorithm follows.

- Compute a histogram of the sample values. That is, count the number of occurrences of each integer between 0 and 255 in the samples in the interval.
- Let  $T$  step from 0 to 255. At each point:
  - Compute the mean and the RMS of the subset of the histogram less than  $T$ .
  - If the RMS is less than 0.25, set  $P$  to be the mean, and continue to the next point.
  - If the RMS is greater than 0.25, define the pedestal to be the last value set as  $P$ , and stop.

Less than 1 percent of the area of a pulse follows the peak by more than 60 ns. Consequently, islands are split at points where the preceding 60 ns are consistent with the pedestal.

### 4 Minimization

The function that is minimized in each fit is the sum of the squared differences between the measured samples and the samples computed from the average pulse shape:

$$R = \sum_{i \in \text{samples}} [S_i - P - \sum_{j \in \text{pulses}} A_j f_i(t_j)]^2. \quad (1)$$

In this expression,  $S_i$  are the measured samples and  $f_i(t)$  is the average pulse shape.  $t_j$ ,  $A_j$  and  $P$  are the fit parameters, representing the times and areas of each pulse and the overall pedestal.

In order to remove any possible dependence on the length of the digitization island, only a subset of the samples is included in the fit. A total of 15 samples are used for each pulse that is included in the fit, ranging from seven samples before the peak through seven samples after the peak. However, samples which equal 0 or 255 are not included since there is no way to know what voltage level they really represent. When several pulses are included in the fit, any of them can cause a sample to be included. The set of included samples is chosen before the minimization process begins based on the initial guess, and it is kept constant during the fit (that is, it is not allowed to change as the pulse times are varied).

For the 1999 data,  $t_j$ ,  $A_j$  and  $P$  were all treated as independent fit parameters, and MINUIT was used for all fits. A refinement of the algorithm was introduced for the 2000 and 2001 data sets which recognizes that only the  $t_j$  need to be included directly as fit parameters; the optimal  $A_j$  and  $P$  can be calculated analytically from them. The partial derivatives of  $R$  in Equation 1 are

$$\begin{aligned} \frac{dR}{dP} &= -2 \sum_{i \in \text{samples}} [S_i - P - \sum_{j \in \text{pulses}} A_j f_i(t_j)] \\ \frac{dR}{dA_j} &= -2 \sum_{i \in \text{samples}} f_i(t_j) [S_i - P - \sum_{j \in \text{pulses}} A_j f_i(t_j)] \end{aligned}$$

The minimum occurs at the point where  $\frac{dR}{dA_j} = \frac{dR}{dP} = 0$ . This condition defines a system of linear equations which may be written in matrix-vector form as  $AX = B$  where

$$X = \begin{pmatrix} P \\ A_0 \\ A_1 \\ A_2 \\ \vdots \end{pmatrix},$$

$$A = \sum_{i \in \text{samples}} \begin{pmatrix} 1 & f_i(t_0) & f_i(t_1) & f_i(t_2) & \cdots \\ f_i(t_0) & f_i(t_0)f_i(t_0) & f_i(t_0)f_i(t_1) & f_i(t_0)f_i(t_2) & \cdots \\ f_i(t_1) & f_i(t_1)f_i(t_0) & f_i(t_1)f_i(t_1) & f_i(t_1)f_i(t_2) & \cdots \\ f_i(t_2) & f_i(t_2)f_i(t_0) & f_i(t_2)f_i(t_1) & f_i(t_2)f_i(t_2) & \cdots \\ \vdots & \vdots & \vdots & \vdots & \ddots \end{pmatrix}$$

and

$$B = \sum_{i \in \text{samples}} \begin{pmatrix} S_i \\ S_i f_i(t_0) \\ S_i f_i(t_1) \\ S_i f_i(t_2) \\ \vdots \end{pmatrix}.$$

For the typical case where there is only one pulse present in the interval being fit, there is only a single fit parameter (the time of the pulse). A simple one-dimensional minimizer is used to optimize it. It assumes that its initial guess is near a parabolic minimum. At each iteration, it computes  $R$  at three points ( $t_0 - 0.2$  ns,  $t_0$ , and  $t_0 + 0.2$  ns), calculates the parameters of the parabola which passes through these points, and determines the position of the minimum. Up to three iterations are allowed. It reports convergence when the time changes from one iteration to the next by less than 0.02 ns. It reports failure if it ever changes by more than 1 ns.

If there is more than one pulse in the fit, or if the simple minimizer fails, MINUIT is used. Its EPS parameter is set to  $10^{-5}$  since this is several times larger than the jump in  $R$  as the fitted  $t_j$  cross the boundary from one 5 ns clock cycle into the next. STRATEGY is set to 0 to request quick-and-dirty computation of derivatives. The parameters to MIGRAD request a maximum of 1000 iterations and determination of the minimum  $\chi^2$  to an accuracy of 10%.

## 5 Initial guesses

The fitting procedure requires initial assumptions for

- the number of pulses present in the interval being fit, and
- their times  $t_j$

The associated pulse areas  $A_j$  and the pedestal  $P$  can then be calculated based on the raw samples and the average pulse shape, as described in the previous section.

The pulses that are initially included are local maxima which exceed a software threshold of 40 ADC counts over the estimated pedestal. Of course, significantly smaller pulses will eventually be found and included, but not in this first iteration.

The first step in estimating the time of the pulse is to compute its “pseudotime”

$$\tau = (2.5 \text{ ns}) \left( i_{max} + \frac{2}{\pi} \tan^{-1} \frac{S_{i_{max}} - S_{i_{max}-1}}{S_{i_{max}} - S_{i_{max}+1}} \right)$$

where  $i_{max}$  is the index of the maximum sample and  $S_i$  is the value of the  $i$ th sample. It should be noted that both the pedestal and the scale of the pulse cancel out in this calculation.

The true time of the pulse is in general a nonlinear function  $t(\tau)$  of the pseudotime. However, for any reasonable pulse shape,  $t(\tau)$  is a monotonically increasing function. The distribution of pseudotimes  $N(\tau)$  can be measured, and the distribution  $N(t)$  of true times is known to be uniform.  $t(\tau)$  is then determined to be

$$t(\tau) = t_o + (5 \text{ ns}) \frac{\int_0^\tau N(\tau') d\tau'}{\int_0^{5 \text{ ns}} N(\tau') d\tau'}$$

The initial guess for each pulse time  $t_j$  is determined from its pseudotime using this formula.

Since the pseudotime is derived from a ratio of integers, the distribution is discretized. In order to remove this purely cosmetic flaw from the final time distribution, the initial guesses are perturbed by a small random number.

## 6 Adding and removing pulses

The decision to add a pulse to the fit is based on local fit quality. Each group of three consecutive samples is examined. The criteria for adding a pulse are (all must apply):

- The residual area must be at least 30 units (approximately 200 MeV).
- The average squared residual of the three samples must exceed 9.
- There must be no other pulse within 2.63 ns.

The initial guess for the time of a pulse that is added is based on the pseudotime computed from the residuals.

There are two sets of criteria for removing pulses that are applied at different stages in the fitting process. At intermediate stages, only pulses that have physically unreasonable parameters are removed. If any of the following properties is met, the pulse is removed:

- The area is less than 20 units (approximately 140 MeV).
- The time is more than 5 ns before the beginning of the interval being fit or more than 5 ns after the end.
- The pulse is within 1.75 ns of another pulse.

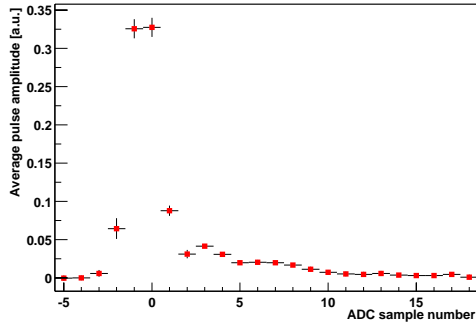
In the final stage, stricter criteria are applied to keep pulses:

- The area must be greater than 40 units (approximately 275 MeV).
- The time must be within the interval being fit.
- There may not be another pulse within 3.5 ns.

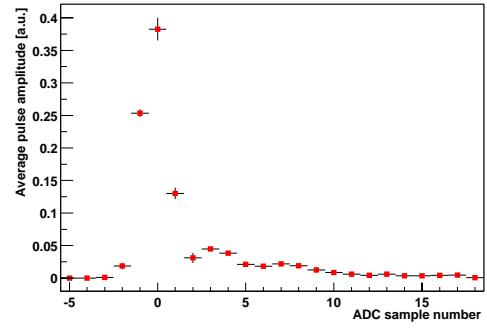
The area and time separation thresholds may appear to be “magic” numbers. In fact, they were obtained with a simple Monte Carlo simulation, which is described in Section 9. The chosen thresholds arose from an iterative application of this simulation. They were first set to very low values and then progressively raised until no spurious pulses were reconstructed.

## 7 Average pulse shape library

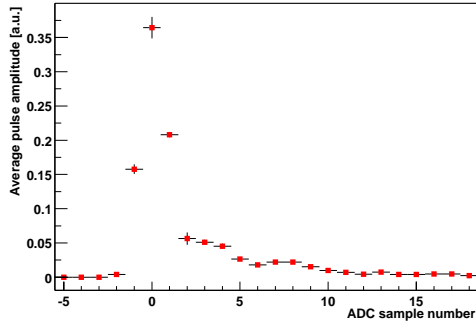
Separate average pulse shapes are built for each detector. The time of a pulse is determined by its peak position, which varies from 0 to 5 ns with respect to the rising edge of the 200 MHz clock which drives the WFD. The pulse shape library is organized into 100 bins along this axis of time relative to the 200 MHz clock. At each of these points, a snapshot is stored of the average pulse shape for pulses at that particular time offset. Examples of these snapshots are illustrated in Figure 1. Each snapshot holds 24 samples, starting 5



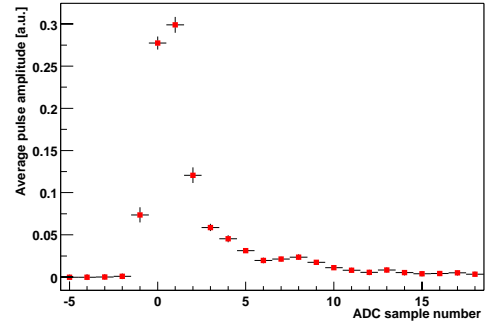
(a)  $t = 0$  ns



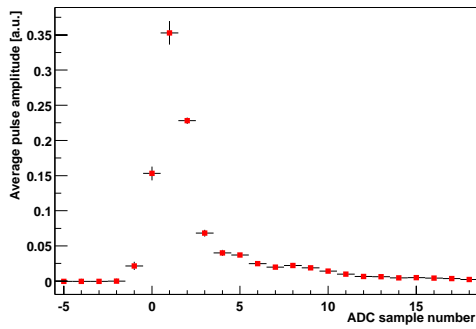
(b)  $t = 1$  ns



(c)  $t = 2$  ns



(d)  $t = 3$  ns



(e)  $t = 4$  ns

Figure 1: A few snapshots from the pulse shape library for station 1 in the 2000 run. Each snapshot shows how a pulse at a given time offset  $\Delta t$  from the 200 MHz clock boundary is sampled (on average) by the WFD. The pulse shape library for each detector contains 100 of these snapshots.

samples before the peak of the pulse and going through 18 samples after. The snapshots are normalized to an area of 1.

The pulse shape snapshots from different offset times can be interleaved to show the overall pulse shape, as shown in Figures 2 through 3. These snapshots should be directly comparable to those from G2OFF.

The pulse shapes were determined from the following runs:

- 1999 data: 4330, 4331, 4333, 4334, 4335, 4341, 4343, and 4347
- 2000 data: 6288, 6614, and 7326
- 2001 data: 11229

Standard quality cuts are applied to remove laser fills, fills with potential quadrupole sparks, and so on. To eliminate pileup, only pulses later than 200  $\mu\text{s}$  after the marker pulse (approximately 145  $\mu\text{s}$  from injection) are used. A pulse area cut from 300 to 350 counts (approximately 2.1 to 2.5 GeV; this varies significantly by detector) is also applied. This is rather arbitrary, since one of the fundamental assumptions of the entire procedure is that the pulse shape is not a strong function of energy. For the 2001 data, the pulse shapes from several different runs were compared and found to be in good agreement.

The pulses which are used to build the pulse library must be aligned in time and normalized to have unit area. The time alignment is particularly critical; if an incorrect procedure is used to determine the time, then the resulting average pulse shape will be distorted. The area normalization is almost irrelevant, since the pulse shape is not a strong function of energy. The pedestal is estimated using the method described in Section 3 in connection with breaking up long digitization islands. The time is estimated with the pseudotime method in Section 5. The area is computed simply by adding together the 16 pedestal-subtracted samples starting 4 samples before the peak of the pulse.

Building the average pulse shape library requires two passes through the data. During the first pass, the distribution  $N(\tau)$  of pseudotimes is constructed. The second pass actually builds the pulse library.

## 8 Cancellation of very low-energy pulses

One of the properties of a pulse finder is that pulses with an energy below a certain software threshold cannot be reconstructed. The reason to have this threshold is to avoid reconstructing noise on the WFD trace as a small pulse. However, true small pulses remain undetected in this case as well. Depending on where these small pulses occur, whether close to a large pulse or far away from it, the effect they have on the large pulse varies.

When a small pulse is close to a large pulse, it will be absorbed in the large one, thereby raising the energy of the large pulse and possibly shifting its time. If a small pulse is far away from the main pulse, it will be absorbed in the pedestal, thereby raising the pedestal by some amount, which in turn leads to a lowering of the energy of the main pulse. By how much the pedestal is affected depends on the length of the island under consideration.

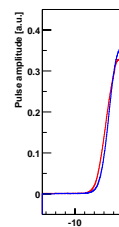
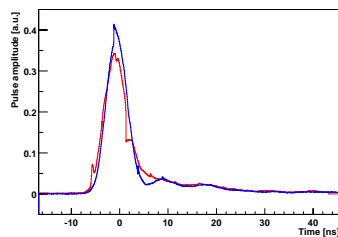
In an ideal case, the energy contributed by small pulses exactly cancels out when averaged over many fills. The proof [5] of this result follows from three assumptions:

- Small pulses are equally likely to appear at any time separation from the large pulse. This is certainly true for suitably small time separations.
- The pulse time is not allowed to vary in the fit. This is true for most pulses in G2OFF FIT, but never exactly true for *MilliFit*. The effect of a small pulse on the pulse time is, however, small.
- A constant is used for the denominator in the computation of  $\chi^2$ , so that the procedure reduces to a least-squares fit.

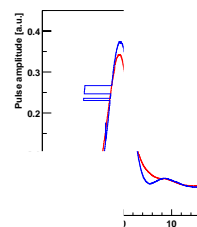
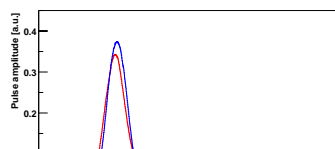
We may simplify the expression in Equation 1 for the typical case of a single pulse over the hardware threshold:

$$R = \sum_{i \in \text{samples}} [S_i - P - Af_i(t)]^2.$$

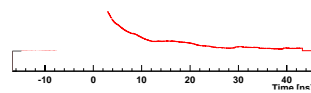




(b) Station 2



(f) Stat



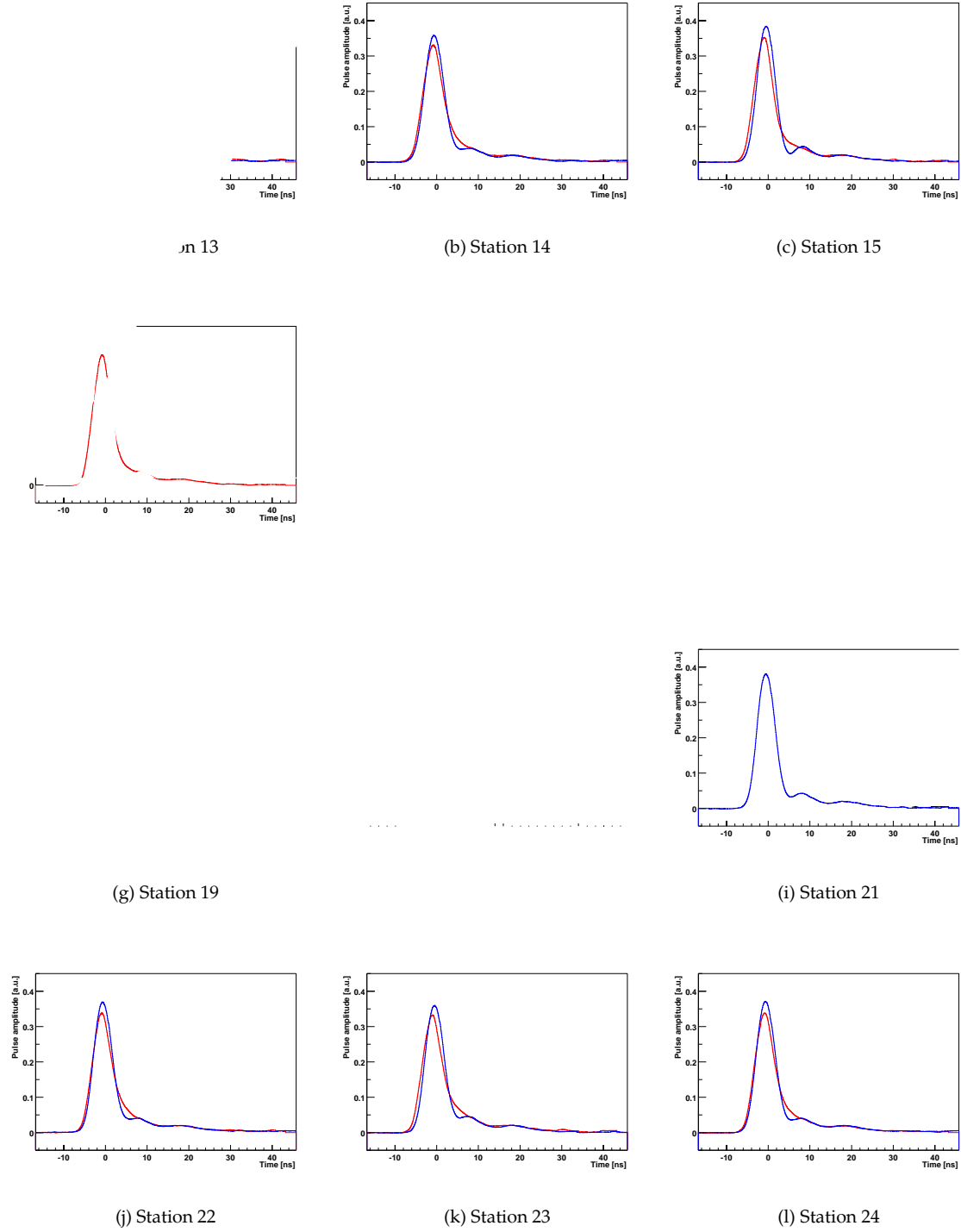


Figure 3: Average pulse shapes from the 2000 data in detectors 13 through 24. Phase 0 is shown in blue and phase 1 is shown in red; alternatively, phase 0 is the shape with more pronounced oscillatory behavior.

Then the solution for the minimum is

$$A = \frac{(\sum_i S_i)(\sum_i f_i(t)) - N_{samples} \sum_i S_i f_i(t)}{(\sum_i f_i(t))^2 - N_{samples} \sum_i (f_i(t)^2)}$$

If a sample  $S_k$  is perturbed by an amount  $\delta S_k$  then the fitted area is perturbed by

$$\delta A_k = \delta S_k \frac{\sum_i f_i(t) - N_{samples} f_k(t)}{(\sum_i f_i(t))^2 - N_{samples} \sum_i (f_i(t)^2)}$$

It should be clear that  $\sum_k \delta A_k = 0$  if the perturbation  $\delta S_k$  is the same for all samples.

In spite of this cancellation, the presence of small pulses causes an increased energy resolution. Consequently, the energy resolution changes from early to late times. A procedure for evaluating the systematic uncertainty in  $\omega_a$  from this effect is given in [3]. There is a potential early-to-late average time shift as well, but it is minimized by choosing a range of samples that is symmetric about the peak of the pulse to be used in the minimization.

## 9 Monte Carlo tests

The system has been tested with a Monte Carlo simulation. It samples the pulse shape to generate raw WFD events containing a set of pulses of known times and areas. It is used to superimpose two pulses from the pulse shape library, fit the resulting waveform, and compare the result with the known input parameters. The figures that are presented here were all generated from a set of  $2 \times 10^6$  events from the simulation.

Figure 4(a) shows the probability that *MilliFit* reconstructs two pulses as a function of the separation in time between the two pulses, broken down into energy bins. All energies follow a similar pattern; for separation times less than 2 ns, essentially no double pulses are reconstructed. For separation times greater than 4 ns, two pulses are essentially always found. In the region between 2 and 4 ns, there is a gradual transition between these two states. Because two pulses are not allowed to have a reconstructed time separation of less than 3.5 ns, double pulses found in this transition region must have (often grossly) misreconstructed times. The individual energies of the two pulses are similarly mistreated. It is found that the individual times and energies can only be trusted for pulses with a separation of at least about 5 ns.

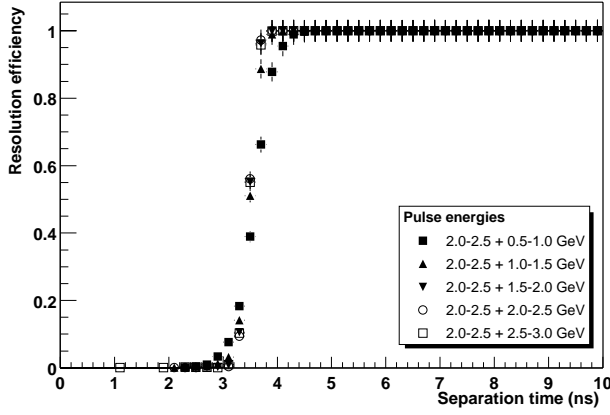
The energy-weighted average time and the sum of the energies are treated reasonably by the algorithm, even for pulses in the transition region. Figure 4(b) shows the ratio of the sum of the energies in all pulses reconstructed by the fitter to the sum of the true energies of the two pulses created by the simulation. It deviates from 1 by as much as 15 percent percent in the transition region; averaged over all unresolvable pileup events, the ratio is 0.94. This necessitates a correction at the histogram-building phase of the analysis.

These corrections (called “Logashenko factors”) are computed for all combinations of overlapping pulse energies  $E_1$  and  $E_2$ . Figure 5(a) shows the average Logashenko factor versus these energies. The factor depends strongly on the separation  $\Delta t$  between the two pulses that are combined. Figure 5(b) illustrates this point by showing the distribution of Logashenko factors obtained for a pair of 2 GeV particles over the entire range of  $\Delta t$  values. Histograms like this one are constructed for every pair of energy ranges  $E_1$  and  $E_2$ ; when simulated pileup is generated, a value is drawn at random from the appropriate distribution.

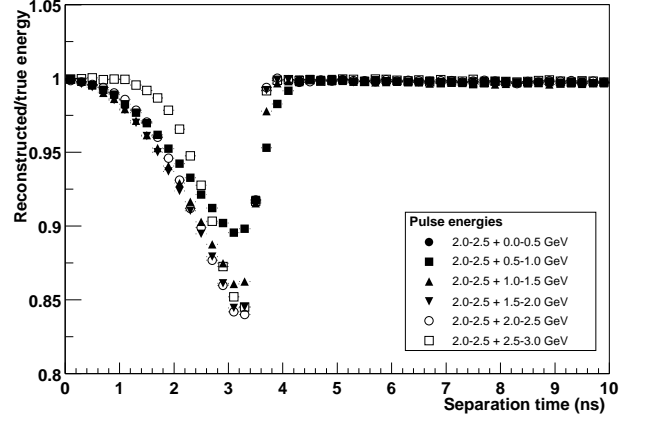
Figure 4(c) shows the difference between the energy-weighted average time of all pulses reconstructed by the fitter and the energy-weighted true time of the two pulses created by the simulation. It deviates from 0 by a maximum of 150 ps in the transition region, which is not enough to require a correction.

The level of cancellation of the effects of small pulses below the software threshold was also estimated from the simulation. Figure 6 shows the ratio of the reconstructed to the true energy as a function of the location of a small pulse with respect to the main pulse. Of course, what matters is the average over the time bins in each of these plots: the extent by which it differs from 1 measures the amount of non-cancellation of the low-energy pileup. These averages are given in Table 1.

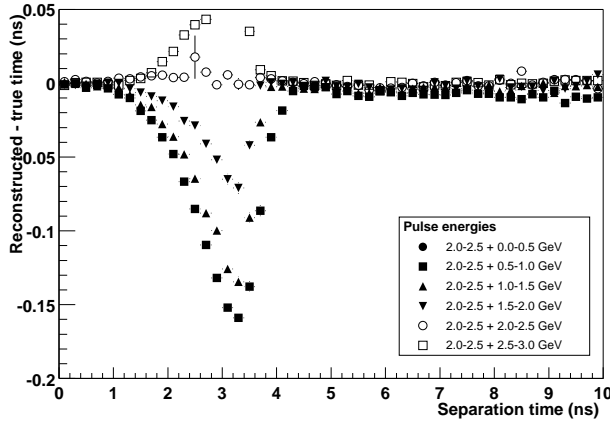
The simulation was further used to examine the behavior of the pulse fitter for very large pulses. The response is linear to within about 1 percent, as shown in Figure 7. It must be noted that this procedure assumes the pulse shape remains the same for these large pulses. The intent of this procedure was to test the sensitivity of the pulse fitter to overflow samples (which are not used in the fit).



(a) Reconstruction efficiency



(b) Reconstructed / true energy

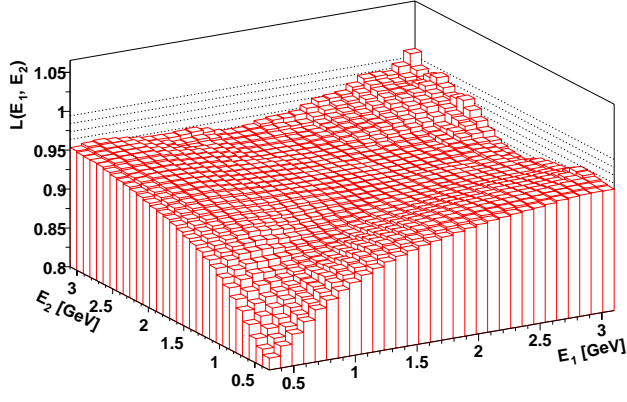


(c) Reconstructed - true time

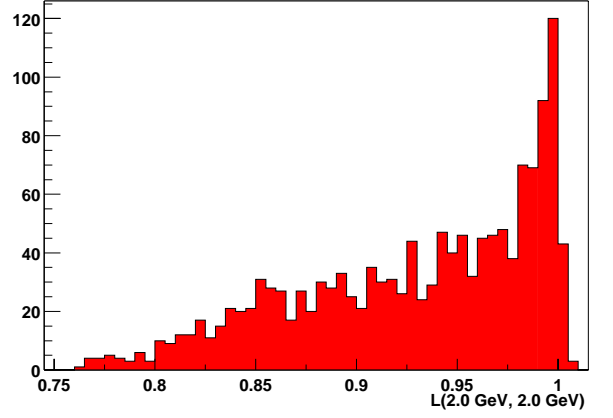
Figure 4: Monte Carlo study of the reconstruction efficiency, the ratio of reconstructed to true energy, and the shift between true and reconstructed time for the MilliFit algorithm as a function of separation time.

Energies	$\Delta E/E$
1.0 + 0.00-0.05 GeV	$2.1 \times 10^{-3}$
1.0 + 0.05-0.10 GeV	$1.7 \times 10^{-3}$
1.0 + 0.10-0.15 GeV	$1.6 \times 10^{-3}$
1.0 + 0.15-0.20 GeV	$2.1 \times 10^{-3}$
1.0 + 0.20-0.25 GeV	$2.6 \times 10^{-3}$
2.0 + 0.00-0.05 GeV	$6 \times 10^{-4}$
2.0 + 0.05-0.10 GeV	$1.6 \times 10^{-3}$
2.0 + 0.10-0.15 GeV	$1.5 \times 10^{-3}$
2.0 + 0.15-0.20 GeV	$1.5 \times 10^{-3}$
2.0 + 0.20-0.25 GeV	$3.0 \times 10^{-3}$

Table 1: This table shows the average over all separation times of the relative influence of low-energy pileup.



(a) Average Logashenko factor versus pulse energies.



(b) Distribution of Logashenko factors for 2.0 GeV + 2.0 GeV pulses

Figure 5: Logashenko factors  $E_{reconstructed}/E_{true}$  for station 19 in the 2000 data.

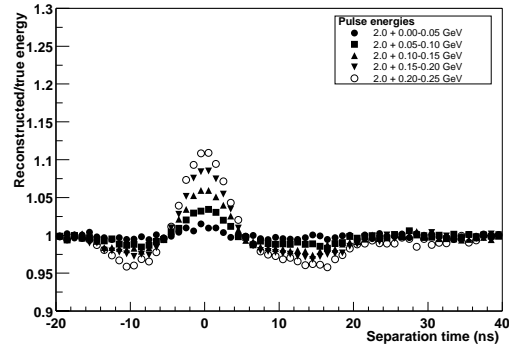
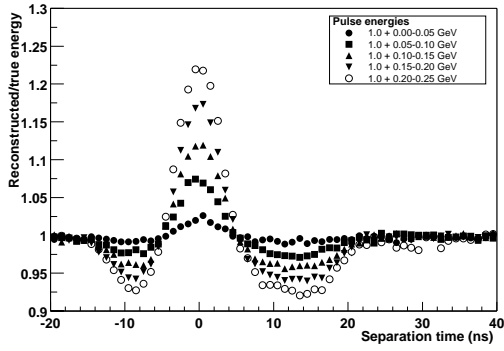


Figure 6: This figure illustrates the effect of small pulses on the energy of 1 GeV (left) and 2 GeV (right) pulses.

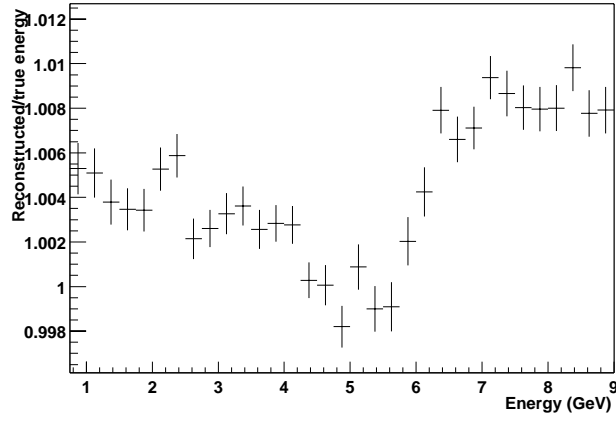


Figure 7: This figure shows the “gain” of the fitter as a function of energy.

## References

- [1] I. Logashenko, “FIT Pulse Finding Algorithm.” Muon ( $g - 2$ ) note 334.
- [2] I. Logashenko, “Shapes of WFD Pulses and the FIT Pulse Finding Algorithm.” Muon ( $g - 2$ ) note 369.
- [3] W. Morse, “The Low Pulse Height Pile-Down Effect.” Muon ( $g - 2$ ) note 373.
- [4] I. Logashenko, “G2OFF-Based Production of 99 Data. Results from Simulation.” Muon ( $g - 2$ ) note 378.
- [5] I. Logashenko and R. Carey, private communication.